Numer Algor
DOI 10.1007/s11075-010-9390-0

ORIGINAL PAPER

Spectral element methods on unstructured meshes: which interpolation points?

Richard Pasquetti · Francesca Rapetti

Received: 13 November 2009 / Accepted: 19 April 2010

Abstract In the field of spectral element approximations, the interpolation points can be chosen on the basis of different criteria, going from the minimization of the Lebesgue constant to the simplicity of the point generation procedure. In the present paper, we summarize some recent nodal distributions for a high order interpolation in the triangle. We then adopt these points as approximation points for the numerical solution of an elliptic partial differential equation on an unstructured simplicial mesh. The L^2-norm of the approximation error is then analyzed for a model problem.

Keywords Spectral elements · Simplicial meshes · Lebesgue constant · High-order interpolation

Mathematics Subject Classifications (2010) 65M60 · 65M70 · 41A05

1 Introduction

High quality polynomial interpolation of functions is a classical topic in approximation theory. It plays an essential role in the success of spectral and *hp*-finite elements applied for the numerical solution of partial differential equations. As soon as the exact solution is smooth, these methods can achieve

R. Pasquetti · F. Rapetti (✉)
J.A. Dieudonné, U.M.R. 6621, C.N.R.S., Université de Nice Sophia-Antipolis,
Parc Valrose, 06108 Nice cedex 02, France
e-mail: frapetti@unice.fr

R. Pasquetti
e-mail: rpas@unice.fr

Published online: 19 May 2010

spectral convergence of the discrete solution by allowing p-refinement of the polynomial degree in each element. While hierarchical hp-finite elements employ modal basis functions (see [21, 24]), spectral element methods on quadrilateral/hexahedral elements (QSEM) employ a nodal approach based on the tensor product of one-dimensional Gauss–Lobatto–Legendre (GLL) points (see, e.g., [2, 8, 15]). The need to extend spectral element formulations to complex geometries and unstructured meshes has recently led to the construction and study of triangular/tetrahedral spectral elements (TSEM); see, e.g., [13, 14, 25, 26] and the previous studies of interpolation nodes on triangles [7, 13].

The question of how to distribute nodes in a triangle or tetrahedron which are suitable for high-order polynomial interpolation is still a somewhat open question. There has been several attempts to produce nodal sets using direct and indirect methods to minimize their Lebesgue constant.

Two factors figure prominently in the quality of high-order polynomial approximations, namely, the smoothness of the function to be interpolated, and the locations of the interpolation points. Interpolations using uniformly distributed points yield undesirable behavior (oscillations) even for analytic functions as soon as the polynomial degree of approximation increases. The problem of how to distribute interpolation nodes in tensor-product domains is solved by recurring to Gauss-Lobatto points. It was not clear how to extend these points to a non-tensor-product domain. Before going into the details, we would like to make a bit of history on some important achievements.

A first widely adopted approach was proposed in [15], based on the idea of using a change of coordinates to transform the quadrangle (and its quadrature points) into the triangle. The main drawback of this approach is that the interpolation points are not symmetrically distributed over the triangle and accumulate at one of the vertices. An early different approach [5] on a triangle was to choose the nodal set which maximizes the determinant of the Vandermonde matrix defined using a suitable L^2-orthogonal polynomials on the triangle up to the 7th order. The resulting nodes are referred to as Fekete nodes. Since Fekete points are known to be the GLL points on the line [10] and in the d-dimensional cube [4], Fekete points are one possible generalization of GLL points for the triangle. This approach was improved and extended up to degree 13 in [7] and further extended to the 18th order in [26]. Note however that the polynomial space used for the d-dimensional cube is different from that used for simplices. In fact, N denotes, on cubes, the maximal polynomial degree in each variable and, on simplices, the total polynomial degree.

An alternative approach was adopted in [13]. It was observed in [23] that the location of the maxima of certain Jacobi polynomials in the interval $[-1, 1]$ correspond to the equilibrium positions of a system of repelling electric charges constrained to lie in the interval. As a consequence, GLL points coincide with the equilibrium positions of these electric charge systems. This analogy has been extended to compute node distributions in the triangle by looking for equilibrium positions of charges distributed in the triangle with line charges fixed on the boundary of the triangle.

Rather recently, different strategies have been adopted with respect to the one discussed so far about nodal distributions resulting from optimizing the interpolation quality of nodes by varying their location. Of great practical interest, especially in three dimensions where optimization procedures become quite complicated (and a natural question arises for non-convex problems: "Is the computed set really the optimal one?"), would be to have an explicit formula for the distribution of points in the triangle/tetrahedron. This was done in [3] and very recently in [11]. Another approach has been proposed in [27], suggesting to replace the task of creating a nodal distribution with a closely related task of building a coordinate transformation for the triangle/tetrahedron, as occurs in the presence of curvilinear finite elements.

We will summarize these most recent existing nodal sets and compare them numerically in terms of Lebesgue constants, generalized Vandermonde matrix conditioning and accuracy when adopted as approximation points in a *T*SEM approach [18] applied to a model problem.

2 Definition of an interpolation grid over a triangle

We consider the interpolation of a function of two variables over a triangular domain T in the xy plane. We suppose this triangular domain to be the image by means of a suitable mapping $g = (g_x, g_y)$ of the reference triangle $T_{\text{ref}} = \{(r, s) : \ -1 \le r, s, \ r + s \le 0\}$. The interpolated function is then approximated with a complete Nth-degree polynomial in r and s, i.e., $(f \circ g)(r, s) \approx (I_N(f \circ g))(r, s) = \sum_{k=0}^{N} \sum_{\ell=0}^{N-k} a_{k\ell} r^k s^\ell$, involving $n = (N + 1)(N + 2)/2$ unknown coefficients $a_{k\ell}$. These coefficients are computed by selecting n interpolation nodes (r_i, s_i) over T_{ref} and enforcing the interpolation conditions $(f \circ g)(r_i, s_i) = (I_N(f \circ g))(r_i, s_i)$ for $1 \le i \le n$. To speed-up the interpolation process, we introduce cardinal node interpolation functions $\varphi_i(r, s)$, $1 \le i \le n$, with the properties of φ_i being a polynomial of total degree $\le N$ on T_{ref} and $\varphi_i(r_j, s_j) = \delta_{ij}$, where δ_{ij} is the Kronecker symbol. The interpolating polynomial can be written as $(I_N(f \circ g))(r, s) = \sum_{i=1}^{n} \varphi_i(r, s) f_i$, where $f_i = (f \circ g)(r_i, s_i)$ are the prescribed function values at each of the n nodes. In this light, the interpolation problem reduces to obtaining an expression for each cardinal function φ_i. Note that the nodal basis $\{\varphi_i\}$ depends only on the interpolation nodes (r_i, s_i). Once this is done, the function f itself can be interpolated at any point (x, y) of T using the expression $(I_N f)(x, y) = (I_N(f \circ g))(r, s)$, with $(x, y) = g(r, s)$.

To compute the cardinal node interpolation functions, we introduce a set of n polynomial functions $\{\psi_j\}$ that form a complete base of the Nth-order polynomial space $\mathcal{P}_N$, and introduce the expansion

$$\varphi_i(r, s) = \sum_{j=1}^{n} c_j^i \psi_j(r, s), \tag{1}$$

where c_j^i are unknown coefficients. Enforcing the interpolation conditions, we find that the vector of coefficients $\mathbf{c}_i = (c_1^i, c_2^i, ..., c_n^i)^t$, corresponding to the ith cardinal function, satisfies the generalized Vandermonde system

$$V\mathbf{c}_i = \mathbf{e}_i, \tag{2}$$

where $\mathbf{e}_i$ is the ith unit vector of the canonical basis of $\mathbb{R}^n$. The $(i,\ j)$ entry of the generalized $n \times n$ Vandermonde matrix V is given by $V_{ij} = \psi_j(r_i, s_i)$. Once the solution of the linear system (2) has been found, the polynomial interpolation over the triangle is accomplished. The difficulty of solving the linear system (2) is related to the conditioning of the generalized Vandermonde matrix which is sensitive to the choice of the basis functions ψ_j, and interpolation points (r_i, s_i). In practice, it is convenient to employ a set of polynomial basis functions that enjoy orthogonal or near-orthogonal properties (e.g., the Koorwinder-Dubiner polynomials [9]).

A good measure of the quality of the polynomial interpolation is given by the Lebesgue constant Λ_N, defined as

$$\Lambda_N = \max_{(r,s)\in T_{\text{ref}}} \mathcal{L}_N(r,s), \qquad \mathcal{L}_N(r,s) = \sum_{i=1}^{n} |\varphi_i(r,s)|, \tag{3}$$

where $\mathcal{L}_N$ denotes the Lebesgue function. This function takes value 1 at the interpolation points (r_i, s_i) and reaches maximal values where nodal coverage is poor, as for example between points. The Lebesgue constant is involved in the mesure of how well the interpolation polynomial function $(I_N f)$ represents f over T_{ref}. Let us consider a function $f^* \in \mathcal{P}_N$ which best represents f in the usual maximum norm $||.||_\infty$. Then in general $f^* \neq I_N f$, but of course $f^* = I_N f^*$. Thus

$$\begin{aligned} ||f - I_N f||_\infty &= ||f - f^* + I_N f^* - I_N f||_\infty \\ &\leq ||f - f^*||_\infty + ||I_N||_\infty ||f^* - f||_\infty \\ &\leq (1 + ||I_N||_\infty)||f - f^*||_\infty \end{aligned}$$

where $||I_N||_\infty = \max_{\{||u||_\infty = 1\}} ||I_N u||_\infty = \Lambda_N$, see [7]. This result provides an upper bound which is the worst possible point-wise error for the polynomial interpolant relative to the best possible uniform polynomial approximation available at the same order. Additionally, the Lebesgue constant bounds the polynomial approximation in terms of the nodal function value [6]

$$||I_N f||_\infty \leq \Lambda_N \max_{1\leq i\leq n} |f(r_i, s_i)|.$$

The Lebesgue constant Λ_N is defined only in terms of the cardinal functions which in turn are defined only depending on the nodal positions, regardeless of the basis functions. It is reasonable to try to construct a set of nodes whose Lebesgue constant is as small as possible. By the way, the practical construction of the nodal set as well as its possible extension to 3D and non-triangular shapes are two other important aspects to consider.

2.1 Koornwinder-Dubiner polynomials [9]

In the reference triangle T_{ref}, the following KD polynomials are L^2-orthonormal, where $L^2(T_{\text{ref}})$ is the Hilbert space of square-integrable functions on T_{ref} and inner product $(f, g) = \int_{T_{\text{ref}}} f(r, s)\, g(r, s)\, dr\, ds$:

$$\psi_{ij}(r, s) = c_{ij} P_i^{0,0}\left(\frac{2r + s + 1}{1 - s}\right)\left(\frac{1 - s}{2}\right)^i P_j^{2i+1,0}(s), \tag{4}$$

with the normalizing factor $c_{ij} = \sqrt{(2i + 1)(i + j + 1)/2}$ and $P_i^{\alpha,\beta}(x)$ being the i-th order Jacobi polynomials [1] evaluated at x.

Let us consider now the space $\mathcal{P}_N(T_{\text{ref}})$ of polynomials defined on T_{ref} and of total degree $\leq N$. The $n = (N + 1)(N + 2)/2$ KD polynomials ψ_{ij}, $i, j \geq 0$, $i + j \leq N$ (see Fig. 1 for an illustration with $N = 4$) constitute an orthonormal basis of $\mathcal{P}_N(T_{\text{ref}})$. Hereafter we no-longer use the notation ψ_{ij} but ψ_k, $1 \leq k \leq n$, with any arbitrary bijection $k \equiv k(i, j)$.

2.2 Uniform grid

One way to introduce the definition of uniform grid on a simplicial domain $T_{\text{ref}} \subset \mathbb{R}^d$ is by means of the notion of barycentric coordinates. Let n_i denote the ith vertex of T_{ref}, ordered in some way. Then, $(d + 1)$ real numbers $\lambda_0, \lambda_1, ..., \lambda_d$ such that $\sum_{i=0}^{d} \lambda_i = 1$ determine a point x, the barycenter of the vertices n_i for these weights, uniquely defined by $\sum_{i=0}^{d} \lambda_i (x - n_i) = 0$.

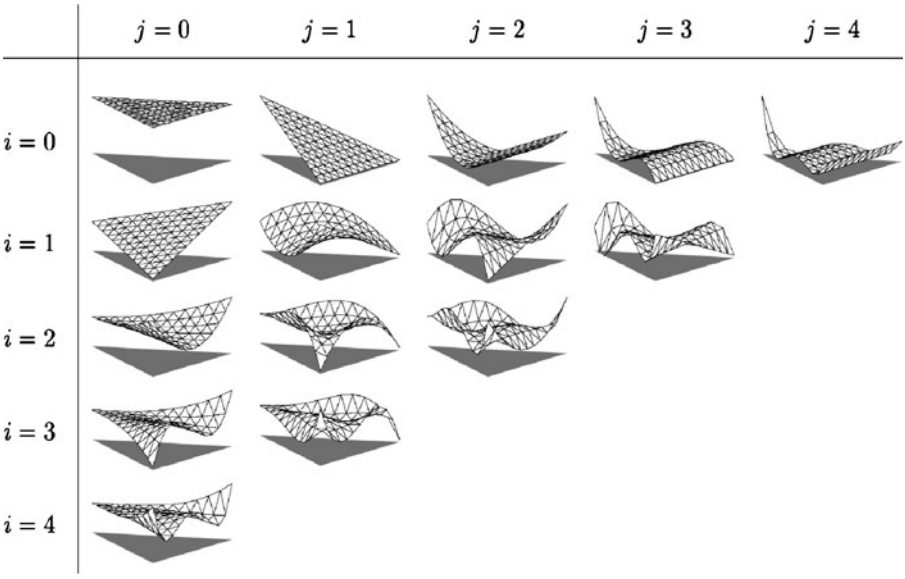

Fig. 1 KD polynomial basis for $N = 4$, taken from [20]

Conversely, any point x has a unique representation of this form, and the weights λ_i are the barycentric coordinates of x in the affine basis provided by the vertices n_i. Note that x belongs to T_{ref} if $\lambda_i(x) \geq 0$ for all i. On T_{ref}, with $n_0 = (-1, -1), n_1 = (1, -1), n_2 = (-1, 1)$, and $x = (r, s)$, we have

$$\lambda_0(r, s) = \frac{1}{2}(-r - s), \qquad \lambda_1(r, s) = \frac{1}{2}(1 + r), \qquad \lambda_2(r, s) = \frac{1}{2}(1 + s).$$

Now, for each integer $N \geq 1$, we define the principal lattice of order N in T_{ref} as the set $\mathcal{T}_N$ of points defined by their barycentric coordinates with respect to the vertices n_i as follows

$$\mathcal{T}_N = \left\{ x \in T_{\text{ref}}, \quad \lambda_i(x) \in \left\{ 0, \frac{1}{N}, \ldots, \frac{N-1}{N}, 1 \right\}, \quad 0 \leq i \leq d \right\}.$$

The uniform grid in T_{ref} associated to the degree N coincides with the nodes of the set $\mathcal{T}_N$. Unfortunately, as the interpolation degree N increases, the accuracy over the uniform grid deteriorates due to the Runge effect. The interpolated function presents large oscillations between the nodes and the Lebesgue constant (see Table 1) as well as the generalized Vandermonde matrix conditioning (see Table 3) increase rapidly with N. As far as it concerns its use within a discretization approach for the numerical resolution of an elliptic problem, it is only suitable for low-order polynomial expansions (see Table 4).

2.3 Fekete grid

A more clever way of arranging the interpolating nodes over the simplex is provided by the Fekete points [26]. To define these points in T_{ref}, we pick a basis $\{\psi_j\}$ for $\mathcal{P}_N$ and we consider the $n \times n$ generalized Vandermonde matrix $V(z_1, z_2, ..., z_n)$ as a function of the nodal positions z_i, and whose elements are $V_{ij} = \psi_j(z_i)$. By definition, Fekete points are the set of points which maximizes the determinant of V within the simplex T_{ref}. Fekete points are independent of the basis choice, since any change of basis only multiplies the determinant by a constant (which is the determinant of the basis change matrix) independent of the points. The Lebesgue constant for these points satisfies $\Lambda_N \leq n$. This fact can be explained by considering the Fekete point cardinal functions. Let us call v the maximum of the determinant of the generalized Vandermonde matrix

Table 1 Lebesgue constants for different nodal distributions on the triangle, for different polynomial degrees N

N	Uniform	Fekete	Lobatto	warp & blend	recursive	approx. Fekete	Sym. [12]
3	2.27	2.11	2.11	2.11	2.11	2.24	–
6	8.75	4.17	3.87	3.70	4.37	6.83	3.87
9	40.92	6.80	7.39	5.74	8.44	12.42	5.59
12	221.41	9.67	17.78	9.36	18.17	19.10	7.51
15	1,315.89	10.02	49.46	17.65	41.74	26.11	9.25
18	8,304.27	14.73	156.22	38.07	113.32	37.99	11.86

$V(\eta_1, \eta_2, ..., \eta_n)$ and let $\{z_i\}$ denote the set of Fekete points which achieves the maximum. The cardinal functions $\varphi_j(z) \in \mathcal{P}_N$ are uniquely defined by $\varphi_j(z_i) = \delta_{ij}$. The Cramer's rule solution of (2) yields the cardinal functions

$$\varphi_j(z) = \frac{detV(z_1, z_2, ..., z, ..., z_n)}{v}$$

where z appears in the jth row. This is because at $z = z_i$, for $i \neq j$, the ith and jth rows of the Vandermonde matrix are equal and then $det(V) = 0$. When $z = z_j$, we have that the determinant of V is at its maximum and thus $det(V) = v$. The expression for φ_j also leads to the bound

$$|\varphi_j(z)| \leq 1, \qquad \forall z \in T_{\text{ref}}.$$

Thus, unlike general optimal interpolation points, Fekete points generate cardinal functions which achieve their maximum in T_{ref} at their associated Fekete point. This property gives a bound on the Lebesgue constant, that is

$$\Lambda_N = \max_{z \in T_{\text{ref}}} \sum_{i=1}^{n} |\varphi_i(z)| \leq n.$$

In the one dimensional case, the bound is well known to be logarithmic in n. Numerical tests suggest that the bound for the Lebesgue constant in the triangle scales like $\sqrt{n} \sim N$, in agreement with the results presented in [26]. Until very recently, the Lebesgue constant for the Fekete points was the lowest known constant for $N > 10$, but in [12, 20] sophisticated optimization techniques have been applied to find nodal sets, starting with Fekete distributions and generating configurations with improved Lebesgue constants (see last column in Table 1, symmetric case).

The computation of Fekete points requires solving difficult optimization problems already at moderate degrees (see [26] where a steepest descent algorithm and explicit formula for computing the gradient of the determinant of the matrix V have been adopted). In some recent papers (see [22] for example) suitable algorithms have been studied, that compute multivariate approximate Fekete distributions by extracting maximum volume sub-matrices from rectangular Vandermonde matrices on any compact domain. These distributions can be defined on elements of any shape but, not being symmetric, they have to be considered, in the absence of a suitable treatment of the points on the boundary, in the framework of non-conforming approaches, such as the nowadays largely studied discontinuous Galerkin element method [11]. In the frame of the conforming *T*SEM discussed here, the approximate Fekete distribution has been modified on the boundary to coincide with the GLL one, in order to recover an usual edge point distribution. Despite this modification on the boundary, the approximate Fekete distribution leads to rather good results.

2.4 Lobatto grid [3]

A competitive alternative to the previous distributions is the one presented in [3]. The proposed grid is generated by deploying Lobatto interpolation nodes along the three edges of the triangle, and then computing interior nodes by averaged intersections to achieve a three-fold rotational symmetry. Let us consider the GLL nodes t_i, $0 \le i \le N$, over $[-1, 1]$, defined as the zeros of $(1-t^2)L'_{N+1}(t)$, where $L'_{N+1}(t)$ denotes the first derivative of the Legendre polynomial of degree $N+1$. Then, we set

$$v_{ij} = \frac{2}{3}\left[t_j - \frac{(t_i + t_{N-i-j})}{2}\right] - \frac{1}{3}, \qquad 1 \le i \le N, \qquad 0 \le j \le N-i.$$

The boundary and interior nodes on T_{ref} are identified by the coordinates

$$r_k = v_{ij}, \qquad s_k = v_{ji},$$

for $0 \le i \le N$, $0 \le j \le N-i$, and $k = k(i, j)$. This configuration is simple to generate, characterized by relatively low Lebesgue constants (see Table 1) and generalized Vandermonde matrix conditioning (see Table 3), and does not compromise the interpolation accuracy (see Table 4).

2.5 Recursive grid

The idea of defining interpolation nodes on concentric triangles was firstly analysed in [6]. The author envisioned a series of concentric triangles of the same arrangement as a uniform grid yet with varying circumradii and then spaced nodes unevenly along each edge. By specifying an edge distribution of Gauss-Lobatto-Legendre points and optimizing the circumradii to maximize the determinant, the author provided Fekete nodes which are exact for $N \le 4$ and approximate for $4 < N \le 7$. An alternative to this construction, which results in a very easy recursive generation algorithm, has been later generalized to arbitrarily shaped domains in [11]. We present it for the triangle with degrees N that are multiple of 3 and we set $m = N/3$. We then consider m concentric triangles, with edges parallel to the ones of T_{ref}, starting from the external one coincident with T_{ref}, and going towards the barycenter $G = (-\frac{1}{3}, -\frac{1}{3})$. Let t_k, $k = 0, 2m$, be GLL points on $[-1, 1]$. The ith concentric triangle is homothetic to T_{ref} with center G and homothety factor t_{2m-i}, $0 \le i \le m$. The last concentric triangle degenerates to the barycenter point G, since for $i = m$ we have $t_m = 0$. On the edges of the ith triangle of the collection, we then define the $3i+1$ GLL nodes. Note that, as expected, the total number of interpolation points is

$$n = 1 + 3\left(\sum_{i=1}^{m} 3i\right) = 1 + \frac{9}{2}m(m+1) = \frac{1}{2}(3m+1)(3m+2) = \frac{1}{2}(N+1)(N+2).$$

Once again, this distribution is characterized by relatively low Lebesgue constants (see Table 1) and generalized Vandermonde matrix conditioning (see Table 3), and does not compromise the interpolation accuracy (see Table 4).

2.6 The *warp & blend* grid [27]

The final construction we consider has its point in the simple observation of the following fact: Given any set of n nodes $\{z_i\}$, it is always possible to construct a mapping g defined on T_{ref} such that the z_i are the images through g of the uniform grid nodes defined in Section 2.2. The question of constructing a set of nodes is then reformulated in terms of constructing such a mapping. To narrow the choice of how the construction of this mapping should be done, the following properties are required:

- The image of the uniform grid nodes on an edge should be the GLL distribution;
- The transform should be bijective;
- The transform should be symmetric with respect to the symmetries of T_{ref};
- The transform should be explicit in barycentric coordinates.

Given the locations t_i of the $N+1$ GLL points on $[-1, 1]$, we construct a one dimensional *deformation* function $w : [-1, 1] \to [-1, 1]$, called the warp function, as the Lagrange interpolant function which interpolates the deformation to the GLL points from the uniform grid points u_j:

$$w(x) = \sum_{i=0}^{N} (t_i - u_i) \prod_{k \neq i, k=0}^{N} \frac{(x - u_k)}{(u_i - u_k)}.$$

They extend the edge warp into the triangle by blending in the edge normal direction, achieving a warp & blend transform g^1 which satisfies the coordinate transform requirements for the considered edge, say edge 1 ($\lambda_0 = 0$). In terms of barycentric coordinates,

$$\begin{aligned} w^1(\lambda_0, \lambda_1, \lambda_2) &= w(\lambda_2 - \lambda_1) v_1, \\ b^1(\lambda_0, \lambda_1, \lambda_2) &= \left(\frac{2\lambda_2}{2\lambda_2 + \lambda_0} \right) \left(\frac{2\lambda_1}{2\lambda_1 + \lambda_0} \right), \end{aligned}$$

where v_1 denotes the unit tangent vector to the edge 1 of T_{ref}, and $g^1 = b^1 w^1$. Constructing analogous transformations on the other two edges, the final coordinate mapping $g = \sum_{i=1}^{3} g^i$. The constraint that the mapping should be isoparametric has been relaxed by introducing a parameter α and considering $g = \sum_{i=1}^{3} (1 + (\alpha \lambda_{i-1})^2) g^i$. The choice of the optimal value for α as well as the programs which construct the points are given in [27]. The (symmetric)

point distribution obtained with this technique performs well, as shown by the obtained numerical results, up to rather high values of the polynomial approximation degree ($N \approx 15$).

3 The model problem and *T*SEM formulation

We now explore how one can construct a spectral element method on non-tensor product domains. Let $\Omega \in \mathbb{R}^d,\ d = 2, 3$, be a bounded Lipschitz domain with piecewise smooth boundary $\partial\Omega$. For simplicity, we consider a model elliptic problem in the plane ($d = 2$), with homogeneous Dirichlet boundary data (although the numerical methods and results presented in this paper can be generalized to three dimensions and to more general elliptic problems):

$$-\mathrm{div}(\alpha\, \mathbf{grad}\, u) + \beta u = f \quad \text{in } \Omega, \qquad u = 0 \quad \text{on } \partial\Omega, \tag{5}$$

where $\alpha, \beta > 0$ are piecewise constant in Ω and f is a given function in $L^2(\Omega)$. We denote by $L^2(\Omega)$ the space of square integrable measurable functions in Ω, and by $H^1(\Omega)$ the space of functions in $L^2(\Omega)$ whose gradient is in $[L^2(\Omega)]^2$. Then let V be the Sobolev space

$$V \equiv H_0^1(\Omega) = \{v \in H^1(\Omega),\ v = 0 \text{ on } \partial\Omega\}.$$

The weak formulation of (5) reads (see, e.g., [19]): Find $u \in V$ such that

$$a_\Omega(u, v) := \int_\Omega \left(\alpha\, \mathbf{grad} u \cdot \mathbf{grad} v + \beta\, u\, v\right) = (f, v)_\Omega := \int_\Omega f\, v, \quad \forall v \in V. \tag{6}$$

The variational problem (6) is discretized by the standard conforming spectral element method, triangle-based (*T*SEM). To this end, we assume that the original domain Ω is decomposed into K triangular spectral elements T_k,

$$\overline{\Omega} = \bigcup_{k=1}^{K} \overline{T}_k.$$

This is a conforming finite element partition, *i.e.*, the intersection between two distinct elements T_k is either the empty set or a common vertex or a common side. Each element T_k is the image of the reference triangle T_{ref} by means of a suitable mapping $g_k,\ 1 \le k \le K$, i.e., $T_k = g_k(T_{\mathrm{ref}})$. Finally, the space V is discretized by continuous piecewise polynomials of total degree $\le N$,

$$V_{K,N} = \{v \in V : v|_{\Omega_k} \circ g_k \in \mathcal{P}_N(T_{\mathrm{ref}}),\ 1 \le k \le K\}.$$

The spectral element approximation of the variational elliptic problem (6) is obtained for the *T*SEM by replacing the L^2-inner product and the bilinear

form defined in (6) with their approximations based on Gauss points. Note that in the classical quadrilateral-based SEM version (QSEM), the GLL points of the quadrilateral are used both as quadrature and interpolation points. In the following we explain why this is no longer possible in TSEM.

Unlike GLL points, a quadrature formula based on the considered interpolation points of the triangle is exact only for integrands in $\mathcal{P}_N(T_{\text{ref}})$. As a result, the spectral accuracy gets lost. Due to this fact, it has been suggested for the TSEM to separate the sets of interpolation and quadrature points, say $\{\hat{x}_i\}_{i=1}^n$ for the first set and Gauss points $\{\hat{y}_j\}_{j=1}^m$ for the second set, obtained by imposing an exact integration of polynomials, e.g., in $\mathcal{P}_{2N}(T_{\text{ref}})$; see [18]. Given the values of a polynomial $u_N \in \mathcal{P}_N(T_{\text{ref}})$ at the interpolation points, one can set up interpolation and differentiation matrices to compute, at the Gauss points, the values of u_N and of its derivatives, respectively. For instance, denoting by $\mathbf{u}$ the vector of the $u_N(\hat{x}_i)$, $1 \le i \le n$, and by $\mathbf{u}'$ that of the $u_N(\hat{y}_j)$, $1 \le j \le m$, we have $\mathbf{u}' = V'V^{-1}\mathbf{u}$, where $V'_{ij} = \psi_j(\hat{y}_i)$. On a generic triangle $T_k = g_k(T_{\text{ref}})$, the same relation between $\mathbf{u}'$ and $\mathbf{u}$ holds true, provided that $u_i = (u_N \circ g_k)(\hat{x}_i)$ and $u'_j = (u_N \circ g_k)(\hat{y}_j)$. Similarly, in T_{ref} one has $(\partial\mathbf{u})' = W'V^{-1}\mathbf{u}$, where ∂ stands for differentiation with respect to any coordinate and where $W'_{ij} = \partial\psi_j(\hat{y}_i)$. Then, using the chain rule, one can compute derivatives in the generic triangle.

The TSEM thus requires the use of highly accurate integration rules based on Gauss points, which is still an open subject of research for high values of N. At a higher computational price, one can however use integration rules based on Gauss points for the quadrilateral and then map them to T_{ref}; see [15]. On a generic triangle $T_k = g_k(T_{\text{ref}})$,

$$(u, v)_{T_k} \approx (u, v)_{T_k,N} = \sum_{j=1}^{m} u'_j v'_j |J_k^T(\hat{y}_j)| \omega_j,$$

where $\omega_j > 0$, $j = 1, m$, are the quadrature weights and $|J_k^T|$ is the Jacobian of the mapping g_k between T_{ref} and T_k, and in general on Ω,

$$(u, v)_{\Omega,N} = \sum_{k=1}^{K} (u, v)_{T_k,N}. \tag{7}$$

We then obtain a discrete problem

$$a_{\Omega,N}(u, v) = (f, v)_{\Omega,N} \quad \forall v \in V_{K,N}, \tag{8}$$

which can be written in matrix form as a linear system $A\mathbf{u} = \mathbf{b}$. The TSEM matrix A is less sparse than the QSEM one and more ill-conditioned, since its condition number grows as $O(N^4h^{-2})$ rather than $O(N^3h^{-2})$ for $d = 2$, where h denotes the maximal diameter of the mesh elements; see [16].

4 Results

4.1 On the reference triangle

To compute the Lebesgue constant, we introduce a uniform Cartesian grid, calculate the Lebesgue function at the grid nodes and perform a direct search for the maximum. The rough maximum is subsequently refined three times to get a more precise estimation. The 4-level algorithm steps are visualized in Fig. 3.

Table 1 shows the approximated values of the Lebesgue constants for the previously considered distributions of nodes over the triangle T_{ref} (Fig. 2). Concerning the value of Λ_N for $N < 9$, the considered different interpolation sets are similar (apart from the uniform one which gives the worst result). Then, their behavior diverge radically at higher order. To provide much more insight on this, we have analysed the profile and the location of the maxima of the Lebesgue functions, for $N = 9, 12, 15, 18$. The success of a given interpolation set in terms of Λ_N may be rephrased by saying that the cardinal functions should have moderate peaks. This fact holds for Fekete type distributions, such as Fekete, warp & blend, approx. Fekete and those in [12]. For the other considered distributions, the interpolation nodes are loosely packed near the edges and the cardinal functions have peaks higher than 1, as shown in Table 2, thus yielding high value of Λ_N. Note that in [20], the magnitude of a node's cardinal function is used as a mesure of the node's influence on the domain. As a result, particular Voronoi tessellations of the triangle are constructed, and excellent interpolatory points occupy barycentric positions in the tessellation cells. The Lebesgue constants computed in [12] are the lowest known. We can conjecture that a break of the node symmetry at the interior of the triangle yields moderate peaks in the cardinal functions, as shown in Table 2 for the degrees which are available in [12] (see also for

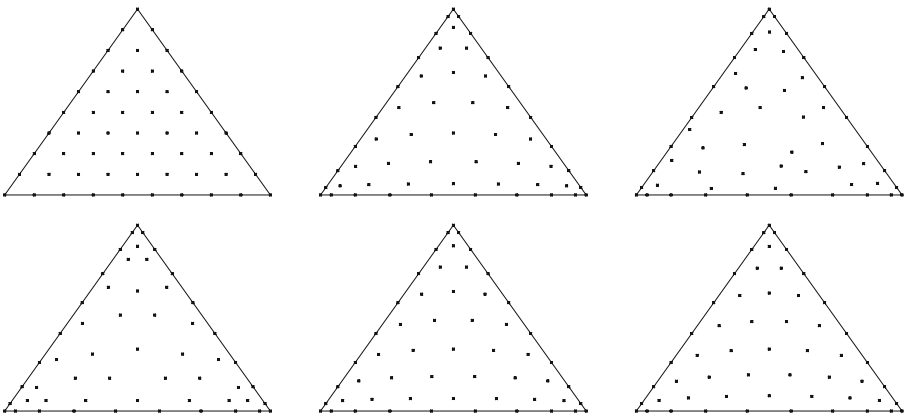

Fig. 2 Node distribution for $N = 9$. *Top line*: uniform (*left*), Fekete (*center*), approximate Fekete (*right*). *Bottom line*: recursive (*left*), warp & blend (*center*), Lobatto (*right*)

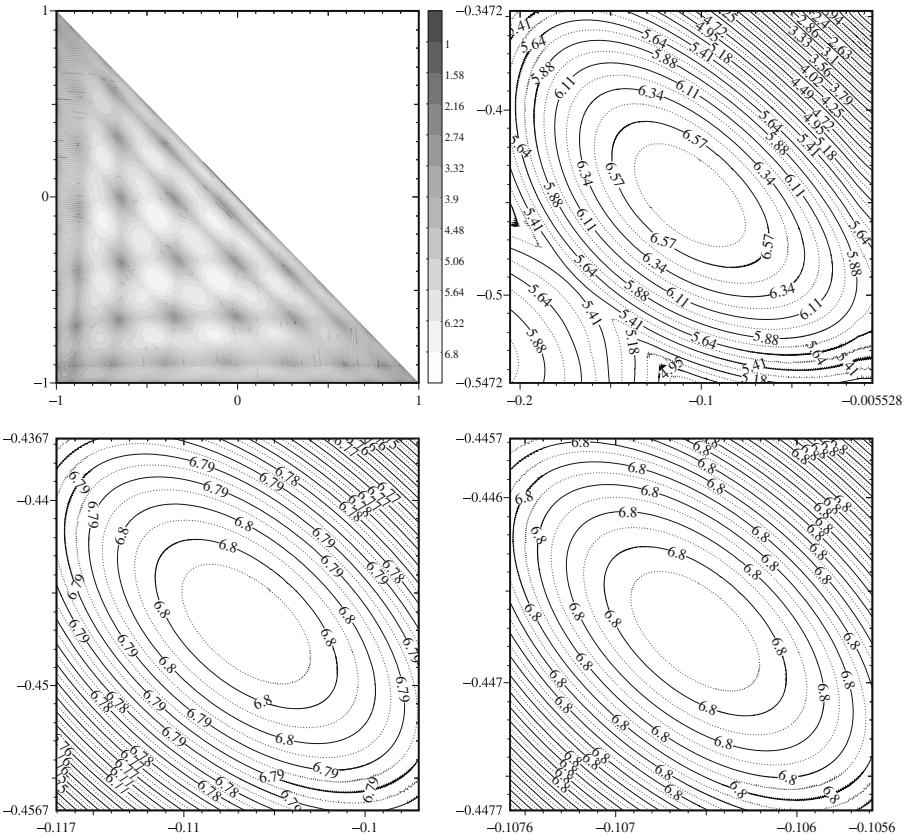

Fig. 3 Results of the 4-level algorithm for the computation of the Lebesgue constant for the Fekete distribution with $N = 9$. Starting from the Lebesgue function value at the grid nodes on the reference triangle (*top line, left*), we refine three times in a square area centered in the rough maximum (colored in *white* on a *greyscale*). At the most refined level (*bottom line, right*), all isolines carry the same value which is the computed Lebesgue constant, here 6.80

the approximated Fekete point distribution when $N = 15$ and $N = 18$ versus the Lobatto or the recursive ones). In Fig. 4 are presented the contour plot of the Lebesgue function on the reference triangle on a grey scale for $N = 12$. As an example, by looking at the warp & blend and Lobatto point distributions,

Table 2 Maximal values of the cardinal functions on the reference triangle computed on a coarse grid

N	Fekete	Lobatto	warp & blend	recursive	approx. Fekete	Sym. [12]
9	1.0	1.0749	1.0120	1.1078	1.2502	1.0480
12	1.0	1.1340	1.0149	1.2010	1.4572	1.1007
15	1.0	2.3020	1.0156	3.1213	1.4434	–
18	1.0	6.6384	1.8257	8.6355	1.3568	–

Note that the true maximal values can be higher than the ones reported here

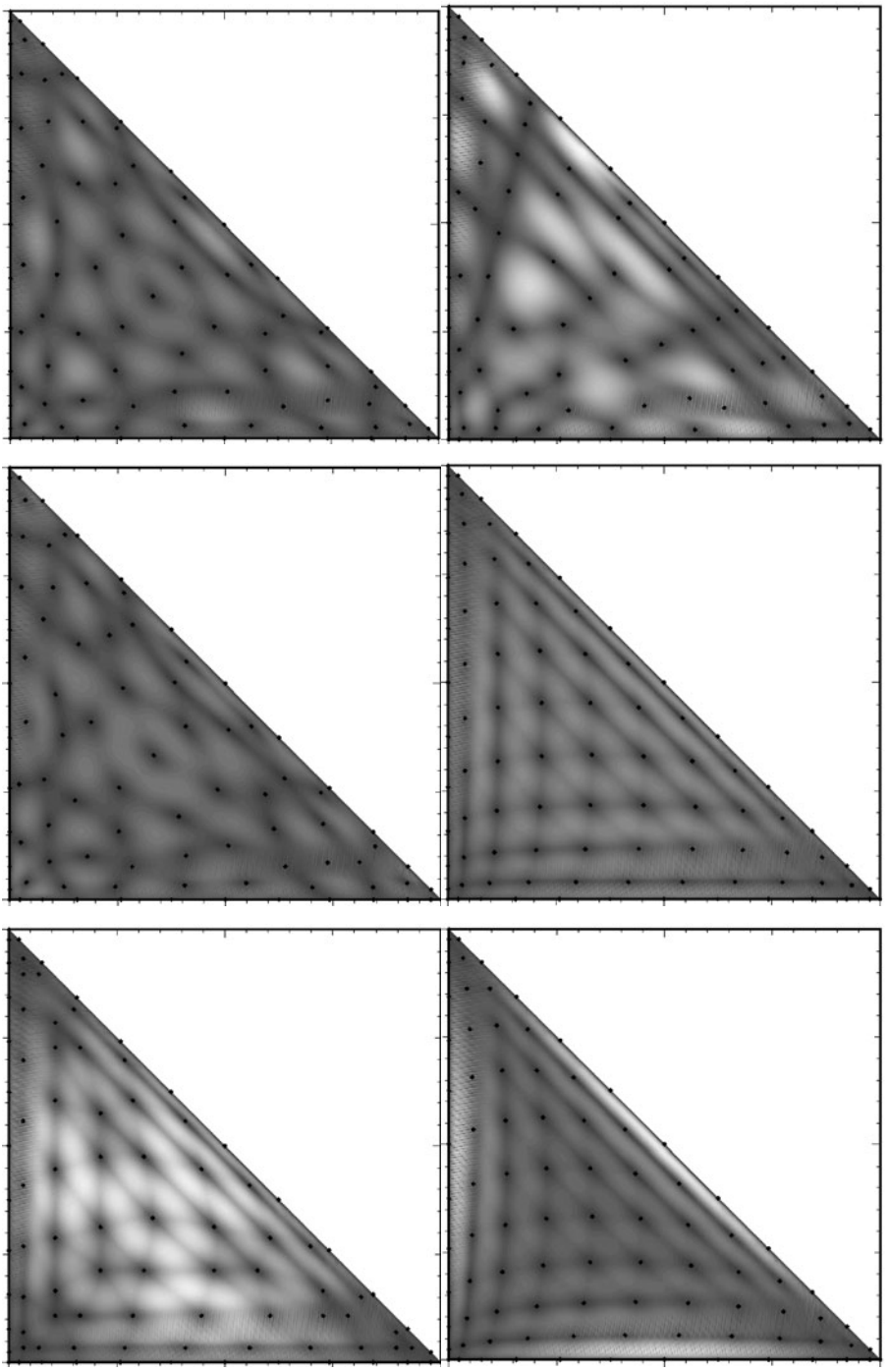

◀ **Fig. 4** Contour plot of the Lebesgue function on the reference triangle associated to, from *top* to *bottom*, Fekete, [12], recursive, on the *left column*, and approximated Fekete, warp & blend, Lobatto, on the *right column*, respectively, with $N = 12$. The *grey scale* is the same for the six plots, from *black* corresponding to 1 to *white* associated to 19, and *black dots* denote the interpolation point locations

it can be observed that peaks form close to the edges for the Lobatto grid thus yielding higher values of the Lebesgue constant.

Furthermore, in Table 3 we report the condition numbers for the generalized Vandermonde matrices built up on the KD polynomials evaluated at the previously considered distributions. As pointed out in Section 2, the condition number of the generalized Vandermonde matrix is important because of the pivotal role that the inverse of this matrix plays in constructing a Lagrange interpolating basis for the nodes.

4.2 On an unstructured simplicial mesh

So far, we have used the Lebesgue constant for nodal sets as an interpolation quality indicator. To further compare the considered nodal sets, we have carried out a convergence test for the *T*SEM applied to the equation $-\Delta u + u = f$, with mixed Dirichlet-Neumann boundary conditions. To this end, we have used the analytical solution $u_{exact} = \sin(2x + y)\sin(x + 1)\sin(1 - y)$ in the domain $\Omega = (-10, 10)^2 \setminus \mathcal{H}$, where $\mathcal{H}$ is a square hole, and Ω is discretized with the unstructured mesh presented in Fig. 5. The source term f and the values for the Dirichlet conditions on the outer boundary and Neumann conditions on the (interior) hole boundary are chosen to match with $u = u_{exact}$.

We recall that the rate of convergence of the *T*SEM with respect to N is essentially determined by s, the smoothness degree of the solution. Thus for $u_{exact} \in H^s(\Omega)$, one can expect the optimal error estimate

$$||u_{exact} - u_N||_{L^2(\Omega)} = O(N^{-s}). \tag{9}$$

Here u_{exact} is analytic and hence we expect to obtain the so-called spectral accuracy, *i.e.*, an exponentially decreasing error as a function of N. Results (Table 4 and Fig. 6) show the the spectral accuracy is achieved with the considered nodal sets, apart of course from the uniform grid set.

Table 3 Condition numbers for generalized Vandermonde matrices formed using the KD polynomials

N	Uniform	Fekete	Lobatto	warp & blend	recursive	approx. Fekete
3	5.8283	5.9028	5.9028	5.9028	5.9028	6.0924
6	14.6583	9.7989	9.8422	9.5912	10.6440	16.6100
9	59.9489	18.1216	18.0994	16.8964	23.3936	23.9434
12	344.9770	22.4680	43.3978	36.1322	71.2535	56.1093
15	2,194.3821	29.4571	130.2558	85.6920	256.1860	92.5440
18	15,597.3340	45.2705	454.6435	224.8035	978.1363	110.8875

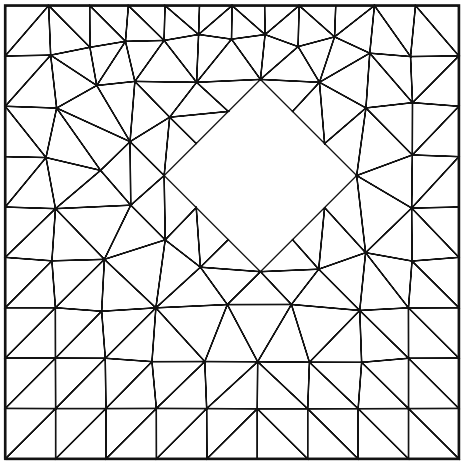

Fig. 5 Unstructured simplicial mesh for the *T*SEM convergence tests. Despite the low number of elements (163) of the mesh, the number of degree of freedom may be considerable, namely 12,042 with $N = 12$ and 26,865 with $N = 18$

Table 4 L^2-norm of the approximation error for different nodal sets

N	Uniform	Fekete	Lobatto	warp & blend	recursive	approx. Fekete
3	5.2655e–0	3.5267e–0	3.5267e–0	3.5267e–0	3.5267e–0	3.9673e–0
6	0.4297e–0	0.1297e–0	0.1565e–0	0.1457e–0	0.1501e–0	0.1447e–0
9	0.3048e–0	5.9582e–3	6.7836e–3	6.3634e–3	5.1638e–3	6.7333e–3
12	0.3146e–0	5.1437e–5	8.9881e–5	9.0467e–5	6.2198e–5	8.4629e–5
15	0.3215e–0	3.6078e–7	8.7952e–7	7.3335e–7	5.0189e–7	5.7335e–7
18	0.3257e–0	1.5364e–9	3.9642e–9	1.0021e–8	4.6452e–9	3.9897e–8

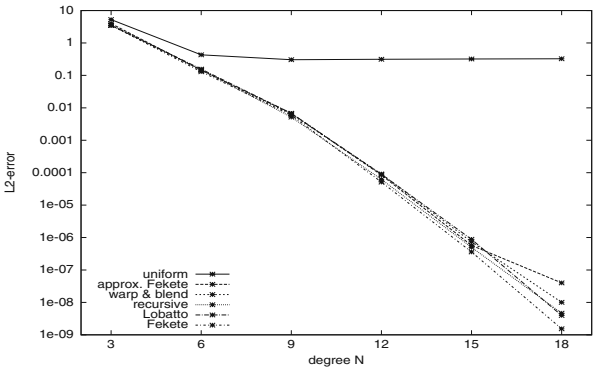

Fig. 6 Semi-logarithmic plot of the L^2-error versus the polynomial order N for different distributions of interpolation points in the mesh triangles

4.3 Conclusions

In the field of conforming spectral element approximation, the treatment of complex geometries requires the generalization to simplicial meshes of the well-known GLL approach on quadrilaterals. The definition of a set of nodal interpolation points is a delicate step in non-tensorial domains as the triangle/tetrahedron. This subject has been widely studied in the last years, and is still open to research. We have presented the most recent constructions proposed by several authors we were aware of, comparing them in terms of Lebesgue constant, Vandermonde matrix conditioning and L^2-error on a model problem.

This selection is certainly non exhaustive. For reasonable values of the polynomial interpolation degree, say $N \leq 10$, these constructions appear rather equivalent and so yields to think that simplicity in the construction should prevail. Note however that the recursive grid [11] could be of special interest when Schwarz overlapping domain decomposition techniques are considered in preconditioning the final algebraic system $A\mathbf{u} = \mathbf{b}$: the overlap is here easy to define, as opposed to what happens with the Fekete [17] and other considered interpolation points. Moreover, the distributions presented in [3, 11, 22, 27] have already been extended to the tetrahedron.

References

1. Abramowitz, M., Stegun, I.A.: Handbook of Mathematical Functions with Formulas, Graphs, and Mathematical Tables. Wiley-Interscience (1972)
2. Bernardi, C., Maday, Y.: Spectral methods. In: Handbook of Numerical Analysis, vol. V. Techniques of Scientific Computing (Part 2), pp. 209–485. North–Holland, Amsterdam (1997)
3. Blyth, M.G., Pozrikidis, C.: A Lobatto interpolation grid over the triangle. IMA J. Appl. Math. **71**(1), 153–169 (2006)
4. Bos, L., Taylor, M.A., Wingate, B.A.: Tensor product Gauss–Lobatto points are Fekete points for the cube. Math. Comput. **70**, 1543–1547 (2001)
5. Bos, L.: On certain configurations of points in R^n which are uniresolvant for polynomial interpolation. J. Approx. Theory **64**, 271–280 (1991)
6. Bos, L.: Bounding the Lebesgue function for Lagrange interpolation in a simplex. J. Approx. Theory **38**, 43–59 (1983)
7. Chen, Q., Babuška, I.: Approximate optimal points for polynomial interpolation of real functions in an interval and in a triangle. Comput. Methods Appl. Mech. Eng. **128**(3–4), 405–417 (1995)
8. Deville, M.O., Fischer, P.F., Mund, E.H.: High-order Methods for Incompressible Fluid Flow. Cambridge University Press, London (2002)
9. Dubiner, M.: Spectral methods on triangles and other domains. J. Sci. Comput. **6**, 345–390 (1991)
10. Fejér, L.: Bestimmung derjenigen Abszissen eines Intervalles für welche die Qradratsumme der Grundfunktionen der Lagrangeschen Interpolation im Intervalle $[-1, 1]$ ein möglichst kleines Maximum besitzt. Ann. Scuola Norm. Sup. Pisa, Sci. Fis. Mt. Ser. II **1**, 263–276 (1932)
11. Gassner, G., Lörcher, F., Munz, C.-D., Hestaven, J.: Polymorphic nodal elements for discontinuous spectral/*hp* element methods. J. Comput. Phys. **228**(5), 1573–1590 (2009)
12. Heinrichs, W.: Improved Lebesgue constants on the triangle. J. Comput. Phys. **207**(2), 625–638 (2005)

13. Hesthaven, J.S.: From electrostatics to almost optimal nodal sets for polynomial interpolation in a simplex. SIAM J. Numer. Anal. **35**, 655–676 (1998)
14. Hesthaven, J.S., Warburton, T.: Nodal high-order methods on unstructured grids. J. Comput. Phys. **181**, 186–221 (2002)
15. Karniadakis, G.E., Sherwin, S.J.: Spectral/*hp* Element Methods for Computational Fluid Dynamics, 2nd edn. Oxford University Press, London (2005)
16. Melenk, J.M.: On condition numbers in hp-FEM with Gauss-Lobatto-based shape functions. J. Comput. Appl. Math. **139**, 21–48 (2002)
17. Pasquetti, R., Pavarino, L.F., Pasquetti, R., Zampieri, E.: Overlapping Schwarz methods for Fekete and Gauss-Lobatto spectral elements. SIAM J. Sci. Comput. **29**(3), 1073–1092 (2007)
18. Pasquetti, R., Rapetti, F.: Spectral element methods on unstructured meshes: comparisons and recent advances. J. Sci. Comput. **27**, 377–387 (2006)
19. Quarteroni, A., Valli, A.: Numerical Approximation of Partial Differential Equations. Springer (1994)
20. Roth, M.J.: Nodal configurations and Voronoi tessellations for triangular spectral elements. PhD thesis, University of Victoria (2005)
21. Schwab, C.: *p*- and *hp*-Finite Element Methods. Theory and Applications in Solid and Fluid Mechanics, Oxford University Press, New York (1998)
22. Sommariva, A., Vianello, M.: Computing approximate Fekete points by QR factorizations of Vandermonde matrices. Comput. Math. Appl. **57**, 1324–1336 (2009)
23. Stieltjes, T.J.: Sur les Polynômes de Jacobi. C. R. Acad. Sci. **100**, 620–622 (1885)
24. Szabó, B., Babuška, I.: Finite Element Analysis. Wiley, New York (1991)
25. Taylor, M.A., Wingate, B.A.: A generalized diagonal mass matrix spectral element method for non quadrilateral elements. Appl. Numer. Math. **33**, 259–265 (2000)
26. Taylor, M.A., Wingate, B.A., Vincent, R.E.: An algorithm for computing Fekete points in the triangle. SIAM J. Numer. Anal. **38**(5), 1707–1720 (2000)
27. Warburton, T.: An explicit construction for interpolation nodes on the simplex. J. Eng. Math. **56**(3), 247–262 (2006)